Optical generation and spatially distinct interferometric detection of ultrahigh frequency surface acoustic waves

D. H. Hurley[a)]
Idaho National Laboratory, P.O. Box 1625, Idaho Falls, Idaho 83415-2209

(Received 8 November 2005; accepted 28 March 2006; published online 9 May 2006)

Generation and interferometric detection of 22 GHz surface acoustic waves (SAWs) using two laterally separated absorption gratings on a Si substrate are presented. Optical phase sensitive detection of SAWs is demonstrated using a modified Sagnac interferometer. The reflection characteristics of the suboptical wavelength grating necessitate the use of only linear polarization. This is accomplished by employing a Faraday rotator to ensure path reversal of the reference and signal pulses. The enhanced sensitivity of the interferometer is exploited to measure the acoustic disturbance on an identical absorption grating at a distance of ~4.5 μm from the generation site. © *2006 American Institute of Physics*. [DOI: 10.1063/1.2203311]

Modulation of electronic and optical properties of semiconductors using highly localized strain gradients has attracted a great deal of attention recently. The applications are many and varied including lateral quantum confinement of carriers using strain gradients associated with patterned stressors,[1,2] acoustic control of recombination pathways,[3] surface acoustic wawes (SAWs) used for finite wave vector spectroscopy,[4] SAW driven single electrons pumps,[5] and electron spin transport using acoustically defined dynamic quantum dots.[6] A motivating factor for this work is the ability to produce lateral modulation of material properties without the problems associated with compositional interfaces. Lateral strain modification of electronic and optical properties typically involves either deformation potential mediated modulation of the conduction and valence band edges[1,2] or the trapping of carriers in the traveling potential wells associated with SAW propagation on piezoelectric semiconductors.[3–6]

While these approaches show great promises they all have limitations. For instance, nanometer scale patterned stressors used to produce static strain gradients mask the carriers underneath.[1,2] Ultrahigh frequency SAWs offer an appealing option since SAW transducers can be patterned far away from the interrogation site.[4,7] However, electrically driven interdigital transducers require a piezoelectrically active material for acoustic wave generation, thus limiting the material systems and crystal orientations that can be investigated.

Optical generation of picosecond SAWs (Refs. 8–10) using nanometer scale absorption gratings provides an attractive alternative to piezoelectric generation. In this letter, thermoelastic generation and interferometric detection of picosecond SAWs using two spatially separate, suboptical wavelength absorption gratings are presented.[11] The work outlined in this letter builds on a previous effort involving generation and detection of picosecond SAWs using a single absorption grating.[10] In that work, SAW detection involved monitoring small changes in reflectivity and as a result of the relatively poor signal to noise ratio; only short, intragrating propagation distances were examined (<1.5 μm). In the present study, it is shown that the enhanced sensitivity provided by the detection of optical phase facilitates the generation and detection of picosecond SAWs on adjacent gratings laterally separated by ~7.5 μm. The samples were prepared using electron beam lithography. They consist of 5 μm long bars periodically deposited on a (100) Si substrate (Fig. 1). The bar axis coincides with the [001] direction. The bar height h, width a, and periodicity p are 50 nm, 110 nm, and 220 nm, respectively. The experimental setup is shown in Fig. 1. The pump and probe pulse trains, derived from the same mode locked Ti:sapphire laser (Coherent Mira 900) with ~1 ps pulse duration and a pulse energy of .06 nJ, are focused at normal incidence onto the sample with a microscope objective producing spot sizes $D \sim 2.5$ μm. In order to take full advantage of the grating bandwidth, the laser pulse duration must be small in comparison to the SAW transit time across one period of the grating. A shaker[12] operated at 12 Hz is placed in the probe (800 nm) leg to provide a variable optical delay. The polarization of the probe pulse relative to the grating axis is varied with a $\lambda/2$ plate. The frequency doubled pump light[13] (400 nm) is amplitude modulated at 1 MHz to facilitate lock-in detection and the polarization plane is aligned with the bar axis.

The detection characteristics of the absorption grating as a function of probe polarization are examined in Figs. 1(b)–1(d). The changes in reflectivity for a uniform, thick aluminum film and a pristine Si substrate are represented in Fig. 1(b) (i) and (ii), respectively. The sharp change in the two signals near $t=0$ is caused by nonequilibrium heating and rapid cooling of the electron gas. These changes are followed by a slow decay caused by thermal diffusion. A comparison between the two detection schemes, optical polarization parallel and perpendicular to the grating axis, is presented in Fig. 1(c). The sign of the thermal response for the parallel and perpendicular detection schemes is of the same sign as the thermal response of the uniform aluminum film and the Si substrate, respectively. This observation illustrates that for the 800 nm probe light the absorption grating acts like a wire grid polarizer with the transmission axis perpendicular to the grating axis.[14] The action of a wire grid polarizer is understood by considering a grating period much smaller than the optical wavelength. In this case the motion of the conduction electrons perpendicular to the grating axis is confined and hence the perpendicular component is essen-

[a)]Electronic mail: david.hurley@inl.gov

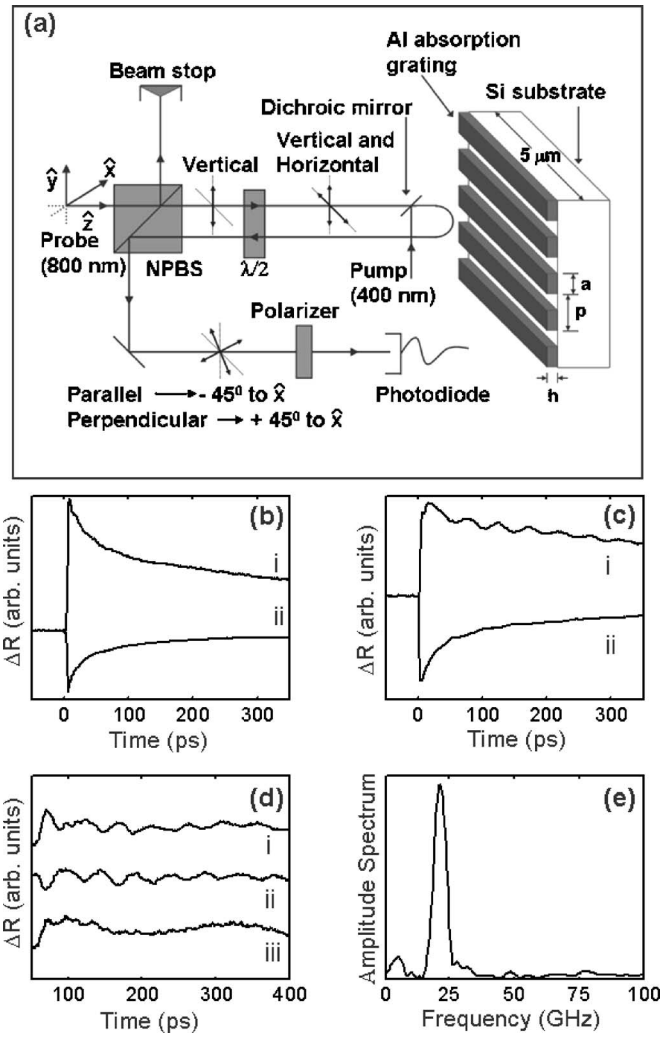

FIG. 1. (a) Experimental setup. (b) Change in reflectivity (ΔR) (i) for a uniform Al film and (ii) for a pristine Si substrate. (c) ΔR for the Al grating; probe polarization is (i) parallel and (ii) perpendicular to the grating axis. (d) Detection characteristic for a probe polarization oriented at 45° to the grating axis. The polarizer passes light with a polarization orientation at (i) +45° and (ii) −45°, to the x axis. The data presented in (iii) are taken without a polarizer. (e) Fourier amplitude spectrum for the data presented in (d) (i).

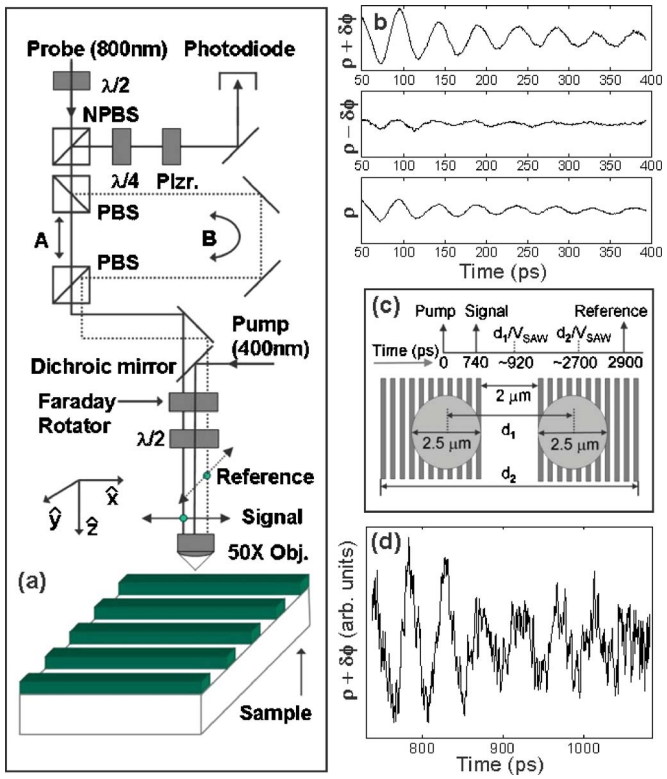

FIG. 2. (a) Schematic of common path interferometer. (b) The interferometric response for $\psi=90°$ (top) and $\psi=0°$ (middle) and the reflectance response obtained without using the polarizer (bottom). (c) Schematic showing the placement of the generation and detection beams on the respective gratings and a time line giving the order of the pulse arrivals and relevant acoustic transit times ($d_1 \sim 4.5$ μm, $d_2 \sim 13$ μm). (d) Interferometric detection of SAWs generated and detected on adjacent gratings.

tially unaltered as it propagates through the grating. To further investigate the detection characteristics, an experiment was performed with an input polarization at 45° to the grating axis, giving components parallel and perpendicular to the grating axis. Upon passage a second time through the λ/2 plate, the parallel and perpendicular components are rotated to an orientation +45° and −45° to the x axis, respectively. These two components are resolved with the aid of a polarizer place before the photodetector [Fig. 1(d)]. The signal components +45° and −45° are out of phase by 180° as a function of delay time. Thus, without a polarizer, both components add destructively[10,15] (iii). There are many mechanisms that contribute to the signal (e.g., photoelastic coupling to the strain field and acoustic modulation of the optical diffraction characteristics of the grating). The relative phase of these contributions as a function input polarization and delay time could account for the phase relation between the +45° and −45° components. The Fourier amplitude spectrum of the data presented in Fig. 1(d) is shown in Fig. 1(e). The center frequency is 22 GHz which corresponds closely to the predicted frequency using the SAW velocity of the substrate material and the grating period, $f=V_{\mathrm{SAW}}/p=22.4$ GHz.[10]

With a basic knowledge of the detection characteristics as a function of input polarization it is now possible to construct an interferometric detection scheme. This approach involves a common path interferometer[16] for monitoring changes in optical phase, Fig. 2(a). The interferometer is composed of two pulses: one that initially traverses path A (signal pulse) and one that initially traverses path B (reference pulse). It should be noted that the reference pulse arrives at the grating approximately 2.1 ns after the signal pulse. This is necessary to ensure that the acoustic disturbance has propagated off the grating before the reference pulse arrives. Typically a λ/4 plate is used to force the normally incident signal and reference pulses to reverse path upon reflection (i.e., ensuring common path operation). However, the reflection characteristics of the suboptical absorption grating, as already discussed, preclude the use of a λ/4 plate which introduces signal components that are parallel and perpendicular to the grating axis. To circumvent this problem, a Faraday rotator was used in place of a λ/4 plate. The Faraday rotator uses an optically active material to rotate the polarization plane. In this case, the polarization state of the light is always linear. A single pass through the Faraday rotator rotates the polarization of both the signal and reference beam by 45°. A λ/2 plate is then used to rotate the polarization plane of the signal and reference pulse to be parallel and perpendicular to the grating axis, respectively. After passing through the Faraday rotator a second time, both beams reverse path and are made to interfere[17] with the

aid of a $\lambda/4$ plate and a polarizer aligned at 45° (in the $\hat{x}+\hat{y}$ direction).

After reflection from the nonpolarizing beam splitter (NPBS) the electric field is expressed as the Jones vector $(E_2 r_s \hat{x} - E_1 r_g \hat{y})$, where r_s is the complex amplitude reflection coefficient of the substrate as seen by the reference pulse (E_2), $r_g = r_g(\tau)$ is the complex amplitude reflection coefficient of the grating as seen by the signal pulse (E_1), and τ is the delay between the pump and signal pulses. (Here z is always along the propagation direction and y is the upward out-of-plane direction.) For monitoring small changes in the real and imaginary parts of the reflectance it is convenient to write

$$r_s = r_{s0}\exp(i\varphi_{s0}),$$
$$r_g = r_{g0}(1+\rho)\exp[i(\varphi_{g0}+\delta\varphi)], \tag{1}$$

where $\rho(\ll 1)$ is the relative change in reflectance and $\delta\varphi(\ll 1)$ is the change in optical phase induced by the pump pulse. If the $\lambda/4$ plate is aligned at an angle of ψ to the y axis, then the intensity at the photodetector for maximum negative, $\psi = 0°$, and positive, $\psi = 90°$, phase sensitivity is given by[16]

$$I_0 \approx E_2^2 r_{s0}^2 + E_1^2 r_{g0}^2 + 2\rho r_{g0}^2 E_1^2 - 2E_2 E_1 r_{s0} r_{g0}\delta\varphi,$$
$$I_{90} \approx E_2^2 r_{s0}^2 + E_1^2 r_{g0}^2 + 2\rho r_{g0}^2 E_1^2 + 2E_2 E_1 r_{s0} r_{g0}\delta\varphi,$$
$$[\sin(\varphi_{s0}-\varphi_{g0})\cos(\delta\varphi) - \cos(\varphi_{s0}-\varphi_{g0})\sin(\delta\varphi)] \approx -\delta\varphi, \tag{2}$$
$$[\sin(\varphi_{g0}-\varphi_{s0})\cos(\delta\varphi) + \cos(\varphi_{g0}-\varphi_{s0})\sin(\delta\varphi)] \approx \delta\varphi.$$

Using published values for the index of refraction for Si and aluminum, the expression $(\varphi_{s0}-\varphi_{g0}) \sim 15°$, validating the linear approximation to the trigonometric identity used in the derivation of Eq. (2). Figure 2(b) shows the two interferometric responses for $\psi = 90°$ (top) and $\psi = 0°$ (middle) as well as the change in reflectance obtained without using a polarizer (bottom). The signal attenuation is primarily due to coupling to bulk modes as the SAW propagates underneath the grating.[9,10] The configuration, $\rho+\delta\varphi$, gives a signal amplitude that is roughly 2.5 times that of reflectance signal alone (bottom).

The final step in this investigation involves generation and detection on two separate absorption gratings. A schematic illustrating the location of the generation and detection spots relative to the two gratings is shown in Fig. 2(c). The grating centers are separated by $\sim 7.5\ \mu$m. The generation and detection pulses irradiate regions near adjacent edges of either grating to minimize the propagation distance between generation and detection spots. It should be noted that it was necessary to minimize the propagation distance under the gratings since SAWs attenuate rapidly in this region due to coupling to bulk modes. The spot size of the pump and probe pulses at the sample surface, $\sim 2.5\ \mu$m, is measured using the gratings as a knife edge. The transit time for a SAW to propagate from the generation to the detection spot centers, $\sim 4.5\ \mu$m, is approximately 920 ps. The interferometic data, $\rho+\delta\varphi$, presented in Fig. 2(d) are for a 0.04 nJ pump pulse and a 0.02 nJ probe pulse. The pump pulse was delayed relative to the signal pulse by 740 ps so that the 920 ps mark fell approximately in the middle of the shaker scan. The signal was average 1000 times to improve the signal to noise ratio. The SAW signal at 22 GHz is clearly revealed. The initial increase and subsequent decay in signal amplitude in Fig. 2(d) is attributed to a convolution of the Gaussian profiles of the probe and the pump as well as acoustic attenuation. Using the signal to noise ratios of the $\rho+\delta\varphi$ signal near $t=0$ and at $t=750$ ps, and assuming a $\sim 0.1\ \mu$rad rad detection resolution,[16] the out-of-plane surface displacement adjacent to the generation grating is estimated[18] to be ~ 1 pm.

In summary, thermoelastic generation and interferometric detection of 22 GHz SAW are demonstrated using two spatially distinct absorption gratings. The reflection characteristics of the suboptical absorption grating necessitate the use of only linear polarization inside the sample interrogation section of the interferometer. A Faraday rotator, which maintains linear polarization throughout, is used in place of a $\lambda/4$ plate to make the normally incident signal and reference pulses reverse path. The enhanced sensitivity of the interferometer is exploited to measure the acoustic disturbance on an identical absorption grating at a distance of $\sim 4.5\ \mu$m from the generation site. Demonstration of remote detection of thermoelastically generated ultrahigh frequency SAWs suggests future experiments that investigate strain modification of the electronic and optical properties in regions that are within the propagation path of the SAWs and adjacent to the generation grating.

[1] K. Kash, B. P. Van der Gaag, D. D. Mahoney, A. S. Gozdz, L. T. Florez, and J. P. Harbison, Phys. Rev. Lett. **67**, 1326 (1991).
[2] I.-Hsing Tan, R. Mirin, V. Jayaraman, S. Shi, E. Hu, and J. Bowers, Appl. Phys. Lett. **61**, 300 (1992).
[3] C. Rocke, S. Zimmermann, A. Wixforth, and J. P. Kotthaus, Phys. Rev. Lett. **78**, 4099 (1997).
[4] I. V. Kukushkin, J. H. Smet, L. Hoppel, U. Waizmann, and M. Riek, Appl. Phys. Lett. **85**, 4526 (2004).
[5] A. M. Robinson, V. I. Talyanskii, M. Pepper, J. E. Cunningham, E. H. Linfield, and D. A. Ritchie, Phys. Rev. B **65**, 045313 (2002).
[6] J. A. H. Stotz, R. Hey, P. V. Santos, and K. H. Ploog, Nat. Mater. **4**, 585 (2005).
[7] Y. Takagaki, P. V. Santos, E. Wiebicke, O. Brandt, H.-P. Schonherr, and K. H. Ploog, Appl. Phys. Lett. **81**, 2538 (2002).
[8] Picosecond acoustics typically involves generation and detection of acoustic waves with wavelengths that are smaller than the optical wavelength of the excitation/detection beams.
[9] B. Bonello, A. Ajinou, V. Richard, Ph. Djemia, and S. M. Cherif, J. Acoust. Soc. Am. **110**, 1943 (2001).
[10] D. H. Hurley and K. L. Telschow, Phys. Rev. B **66**, 153301 (2002).
[11] Suboptical wavelength absorption grating refers to a grating period that is smaller than the optical wavelength of the pump and probe beams.
[12] D. C. Edelstein, R. B. Romney, and M. Scheuermann, Rev. Sci. Instrum. **62**, 579 (1991).
[13] The reflected frequency doubled pump light is efficiently filtered from the reflected collinear probe light using a dichroic mirror [Figs. 1(a) and 2(a)].
[14] B. Stenkamp, M. Abraham, W. Ehrfeld, E. Knapek, M. Hintermaier, M. T. Gale, and R. Morf, Proc. SPIE **2213**, 288 (1994).
[15] Coherent interference involving optical phase is not considered since the two signals have orthogonal polarization vectors.
[16] D. H. Hurley and O. B. Wright, Opt. Lett. **24**, 1305 (1999).
[17] It is important to note that the common path design ensures that the signal and reference beams are temporally coincident after reflection from the NPBS (Fig. 2).
[18] This estimation assumes that the phase contribution to the signal is due purely to out-of-plane surface motion.